Concrete LNG GBS Terminal Ship Collision Study

Fuqiang Wu (M)
Energo Engineering, Inc.

Frank Puskar (M)
Energo Engineering, Inc.

Pascinthe Saad
ConocoPhillips Company

ABSTRACT: A Concrete Gravity Based Structure (GBS) provides an opportunity for the storage of Liquefied Natural Gas (LNG) and represents one of the key elements of an LNG receiving and regasification terminal. The impact resistance of an offshore LNG GBS against accidental ship collision needs to be evaluated. Nonlinear elasto-plastic Finite Element Analysis (FEA) provides a useful numerical tool to assess the damage and evaluate the overall structural integrity of the GBS following a ship collision. In the work presented, a large capacity tanker was modeled using FEA and simulated to collide into a prototype concrete LNG GBS. An efficient, two-step approach was applied to estimate the damage levels caused by the striking tanker considering different approach speeds. Various benchmark tests were conducted to validate the steel and concrete FEA models to ensure the reliability of the analysis. The simulation shows that certain collisions can cause damage to both the tanker bow and the LNG GBS, depending upon the collision speed and the configuration of the colliding bodies. However, these collisions do not always result in a breach of the LNG containment. The results of this type of assessment can be used to assist in designing the LNG GBS to improve its impact resistance. The results can also be used in risk studies typical of these types of facilities.

KEY WORDS: LNG; GBS; CSC; FEA; numerical simulation; ship collision; impact; concrete; damage.

INTRODUCTION

Offshore LNG terminals are a viable solution for importing LNG to meet the ever-growing demand for energy. Of the different types of possible structural configurations, a concrete GBS provides one of the best solutions for the receiving, storage, and regasification of LNG offshore.

In design and operation of the LNG terminals, public safety is a major concern due to the potential consequences of an accidental LNG spill at the terminal location. While a variety of accidental scenarios and conditions need to be considered, a ship colliding into the GBS and its impact to the structure and the LNG tank pose a substantial threat and need to be carefully studied for a safe design.

Compared to steel structures, a concrete GBS system has many advantages. Concrete structures are comparably durable and require less maintenance in marine environment. They have better resistance to cryogenic temperature. Concrete structures are also considered to have stronger resistance against accidental ship collision, fire and explosion (Jiang 2004). Despite a general opinion of strong impact resistant capacity of concrete structures, only limited research and studies have been carried out previously on the behavior of concrete structures under large object impacts (El-Tawil 2005). Even fewer are related to the offshore concrete LNG GBS application.

This paper describes a detailed case study of the ship impact resistance of an offshore LNG GBS, Concrete Storage Caisson (CSC) structure, using numerical simulation techniques. The modeled CSC is a prestressed concrete cylindrical structure providing protective shelter for the LNG tank. A large capacity oil tanker was simulated to collide with the CSC at a 90^{o} "T-bone" position. Elasto-plastic Finite Element Analysis (FEA) was performed in the study to investigate the behavior of the GBS under the impact loads. This case study assisted in the conceptual design of the CSC to improve its collision resistance. It can also provide input to the risk studies typical of similar types of facilities.

SHIP COLLISION MODELING

In recent years, considerable efforts have been directed towards the development of numerical techniques and methodologies to simulate the mechanical response and large amount of energy dissipation in the deformable object collision process. Most of these efforts are related to applications in the military, transportation, aerospace, and automobile industries. With the increasing demand of marine environmental protection, similar collision studies have gradually started to see application in the ship building industry for better hull structural design to resist ship collision and grounding.

Different from traditional analytical approaches, nonlinear elasto-plastic finite element analysis of ship collision problems involves complicated structural modeling and time-consuming numerical simulations. Recent literature indicates various methods and techniques applied in the finite element modeling and simulation of steel ship collision and grounding studies. Some of these are simplified with limitations. Some others are especially complicated and require large amounts of time in both the modeling stage and the simulation stage.

A series of analytical methods and solutions were developed and applied in the last decade (Peterson 1982, Wierzbicki 1992-1999, Puskar and Litton 1993, Simonsen 1997, Pedersen 1998, Paik et al. 1999, Wang et al. 2000, 2003, Suzuki et al. 2000, Brown et al. 2001). And the representative numerical studies of the steel ship collision include Kuroiwa (1996), Kitamura et al. (1998, 2001), Endo and Yamada (2001), Tornqvist (2003), and Wu et al. (2004). These efforts advanced the understanding of ship collisions and damage mechanisms.

Since the colliding structures are highly transient and nonlinear and behave in many complex patterns, modeling this continuous structural interaction requires proper handling of the FEA model and special techniques to simulate the process. Due to the rapid advances in the FEA codes and their application, nonlinear FEA simulation of a ship collision becomes a viable, efficient, and thus practical option. Many powerful FEA packages are capable of solving transient, large deformation, contact, and material nonlinearity problems such as a ship collision, in spite of the challenges to include these features in the simulation.

Of the various challenges in collision simulation, proper modeling of the material properties is the most demanding. A preferred material model should account for the elasto-plastic behavior under multi-axial stress field, the strain hardening effect, the strain rate effect, and the material rupture and damage behavior.

Steel is a better defined material and is less difficult to model compared to concrete. Since concrete has distinct characteristics compared to steel, modeling concrete material to incorporate its plastic, cracking, and damage behavior has been a challenge for many years. A proper concrete model generally requires considerable effort to verify with test data. In this study, significant effort was devoted to the concrete material modeling. Several iterations were required to properly model the reinforced concrete walls to best represent both ductile steel reinforcement and the brittle concrete behavior.

Generally, a real time full dynamic simulation of the ship collision requires very detailed FEA model of the entire ship and extensive simulation time for a single collision scenario. These often exceed the computer hardware capability and the time frame allowed for the project. In this study, a simplified two-step approach was used to solve this problem and make the study efficient and practical.

This approach divides the problem into two separate steps, internal collision mechanics and external collision mechanics. Compared to full dynamic analysis, this two-step approach is very efficient in generating both the structural response and energy dissipation in terms of deformation and damage to the colliding bodies, as well as the estimated collision speeds of the striking vessel, in only one simulation run. In particular the analysis does not have to be run and rerun for a large number of initial collision speeds.

The internal collision mechanics involves one simulation to push the striking vessel (with an assumed speed) into the CSC structure to estimate the structural deformation and failure response of the involved colliding bodies (e.g., bow of striking vessel and side structure of struck facility) and obtain the absorbed energy in the entire collision process in terms of critical steel and concrete failure. The external collision mechanics involves an analytical evaluation of the global rigid body motion of the structures, accounting for the hydrodynamic effect of the surrounding water. By analyzing the external mechanics, the portion of initial kinetic energy that must be absorbed during the vessel and CSC colliding interaction can be computed for the specific impact scenario. In summary, the internal mechanics relates to the energy absorption of the two colliding bodies in terms of material deformation and failure, while the external mechanics relates to the global rigid body motion of the vessels.

CSC CONCRETE STRUCTURE MODEL

The prototype CSC is a reinforced and prestressed cylindrical structure with a base diameter of approximately 80 m and a height of approximately 65 m in a 20 m water depth. It is directly supported at sea bed level and consists of a circular base caisson and the cellar region, comprising a bottom base slab and top LNG tank slab separated by an array of circumferential and radial walls. Fig. 1 shows a conceptual sketch of the CSC centerline cross section.

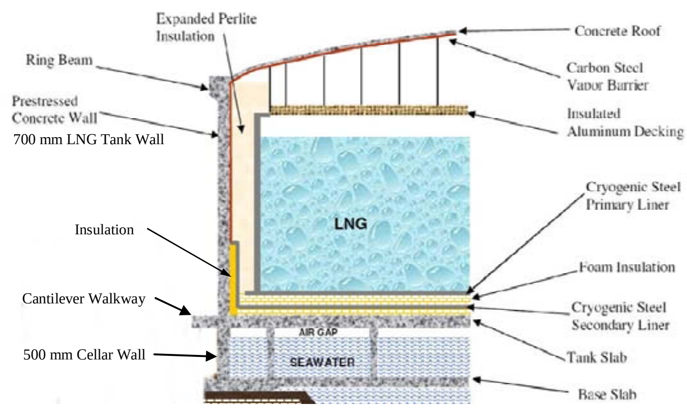

Fig. 1. CSC section schematic

As shown in the figure, the LNG tank consists of the tank containing the LNG, layers of insulation material, and the 700 mm thick prestressed concrete wall as the major protection structure. The cellar region functions to provide buoyancy and ballast and distribute the LNG tank load to the foundation. The concrete tank wall is designed for C50 high strength concrete and heavily reinforced with horizontal and vertical Grade 75 (Fy=520 MPa) steel rebars.

The CSC is a large stationary fixed structure so the structure response under impact loads is generally localized at the contact region. To simplify the problem, only part of the structure (a 75^{o} sector) was modeled. Fig. 2 shows two general views of the resulting finite element model of the CSC. The colors shown in the figure represent different parts or materials.

The FEA model was implemented in the LS-DYNA FEA program. Solid elements were used to model the concrete portion of the CSC. General mesh size for the concrete walls and slabs is approximately 900 x 900 mm. The mesh size is finer in the region of possible contact during ship collision in order to more accurately capture local structural failures at the collision interface. To better model the response of the concrete wall and to reflect the rebar effect, the 700 mm tank wall was divided into 6 layers thru-thickness. The 500 mm cellar wall was similarly divided into 4 layers thru-thickness.

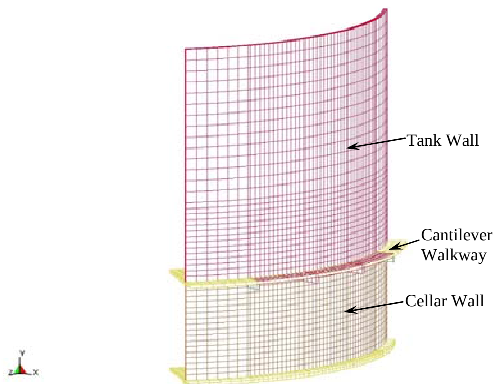

(a) Exterior view

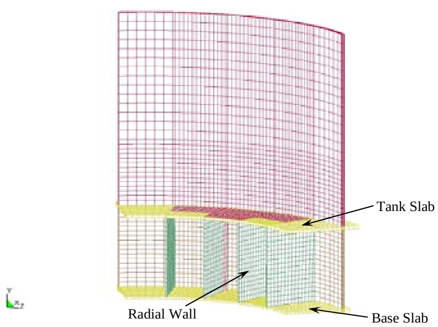

(b) Interior view

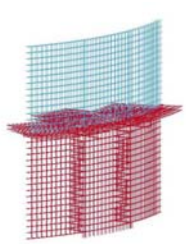

(c) Embedded steel reinforcement grid in concrete

Fig. 2. CSC finite element model

The concrete reinforcement was explicitly modeled, as also shown in Fig. 2. Bar elements were used for rebar modeling. These reinforcing bar elements were embedded in the solid concrete elements. Considering the fast impact loading effect during a collision, the rebar was assumed to be fully bonded with the concrete elements so no bond slip was accounted for between concrete and rebar. This assumption was mainly intended to simplify the CSC model. The effect and sensitivity of concrete and rebar bond slip to the results may be studied at a future date.

The concrete material was modeled using Schwer & Murray Cap Model (LSTC 1998), which is a three invariant cap model including viscoplasticity for rate effects and damage mechanics to model strain softening. The damaged elements, in tension or in compression, can be removed from the model in terms of its resistance contribution to the collision when the damage parameter exceeds a defined value. This allows for explicit modeling of the damage caused to the CSC as the ship collides into the structure. The reinforcement was modeled as plastic kinematic material including strain rate effect and strain failure.

The concrete and reinforcement material properties are listed in Tables 1 and 2. These properties are relatively conservative values for such study. The steel material model was tested before and published in a separate paper (Wu et al. 2004). The performance of the concrete material model was validated through two typical tests, a standard cylindrical compression test and a simple cantilever beam bending test. Both tests reproduced the expected failure mode, a closely matched stress vs. strain curve, and strength value compared to the laboratory test results. Fig. 3 shows a comparison of the laboratory cylindrical compression test and the FEA results.

Table 1. Concrete material properties

Concrete Grade	**Density (kg/m^3)**	**Compressive Strength, f_c' (N/mm^2)**	**Tensile Strength, f_t (N/mm^2)**	**Young's Modulus (N/m^2)**	**Poisson Ratio**
C50	$2.4x10^3$	50	4.1	$3.32x10^{10}$	0.20

Table 2. Reinforcement material properties

Reinf. Grade	**Density (kg/m^3)**	**Yield Strength (N/mm^2)**	**Ultimate Strength (N/mm^2)**	**Rupture Strain**	**Young's Modulus (N/m^2)**	**Poisson Ratio**
Grade 75	$7.85x10^3$	520	690	0.16	$2.0x10^{11}$	0.3

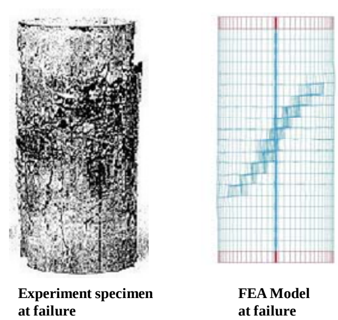

Fig. 3. Concrete cylinder compression test

TANKER MODEL

An Aframax class 105,000 DWT double hull oil tanker was used as the representative striking vessel for this exercise. General particulars for this vessel are presented in Table 3.

Table 3. General particulars of prototype tanker

Description	Values
Length, Overall	245 m
Breath, Moulded	42 m
Depth, Moulded	21 m
Design Draft (laden)	12 m
Full Displacement	125,000 tonnes

To reduce the FEA model size, only the bow section of the striking oil tanker was modeled. The tanker model generally includes the bow structure up to the first transverse oil tight bulkhead forward of the cargo block. In this region, the major structural components were modeled to represent the typical scantlings of this type of vessel and most importantly the typical structural stiffness and arrangement characteristics.

Thin shell elements were used to model the steel plates of the ship shell, decks, bulkheads, frames, girders and other scantlings. General mesh size is approximately 400 mm. Formulation of the shell element includes the shell warping effect. The shell elements were modeled as plastic kinematic material including strain rate effect and strain failure. The steel material model was tested and validated. Details of the validation results can be found in Wu et al. (2004).

Fig. 4 shows the profile and the cut section of the tanker model. The cut section shows the interior detail such as framing, bulkhead and decks. These details as well as plate thicknesses and material properties are generally consistent with those tankers of similar type. The colors shown in the figure represent different plate properties (i.e. different plate materials or thicknesses). The steel material properties used in the tanker model are provided in Table 4.

Table 4. Material properties of tanker scantlings

Steel Grade	Density (kg/m^3)	Yield Strength (N/mm^2)	Ultimate Strength (N/mm^2)	Rupture Strain	Young's Modulus (N/m^2)	Poisson Ratio
AH 32	7.85x10^3	315	515	0.22	2.0x10^{11}	0.3
Mild Steel	7.85x10^3	235	460	0.22	2.0x10^{11}	0.3

COLLISION SIMULATION AND RESULTS

A 90^o "T-bone" collision scenario between the tanker and CSC was investigated. The impact was assumed to occur at the center of one CSC cellar compartment, which is expected to be a weaker part of the cellar region in terms of less involved structural components and maximum possible penetration of the tanker. Full laden draft was assumed for the striking tanker. This impact position is believed to represent the worst case collision scenario related to possible LNG release. Fig. 5 shows the combined CSC and tanker collision model.

(a) General view

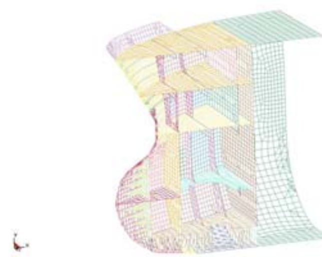

(b) Cut section (centerline bulkhead not shown)

Fig. 4. Tanker finite element model

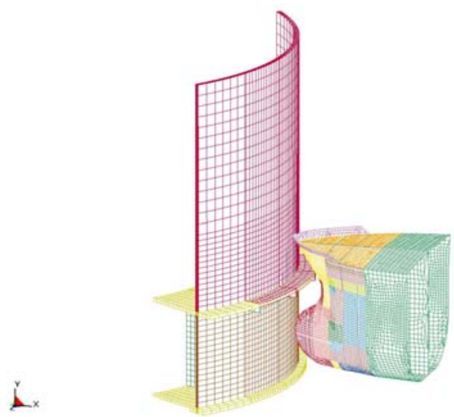

Fig. 5. CSC and tanker collision model

The contact definition of this problem allows the contact to occur between the striking tanker bow and CSC concrete elements and reinforcement bar elements as well as contact between different structural parts on the same vessel (i.e., the different parts of the striking bow structure). Friction effects were also considered and included in the collision model.

This collision numerical simulation technique was verified and benchmarked before by the authors (Wu et al. 2004). The benchmark exercise involved a comparison between the numerical simulation and a laboratory test of a scaled cone and double hull collision.

The CSC gravity, operational loads, hydrostatic pressure, and concrete wall prestress were estimated and applied to the CSC structure as initial pre-load condition. The tanker bow was activated with an initial velocity and was constantly pushed at this speed into the CSC structure. The initial pushing velocity was estimated to be in the approximate range of that expected to breach the CSC.

Simulation results are presented in Fig. 6 as snap shots of CSC and tanker collision at several critical instances.

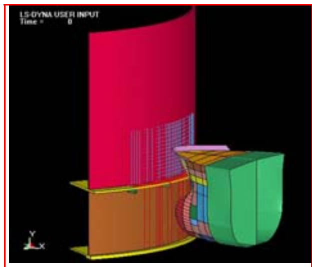

Instance A – CSC and tanker before collision

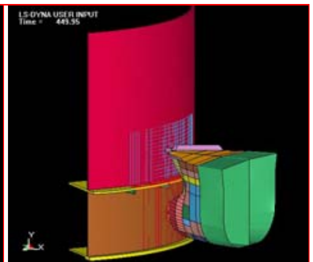

Instance B – Cellar wall initial thru-thickness crack

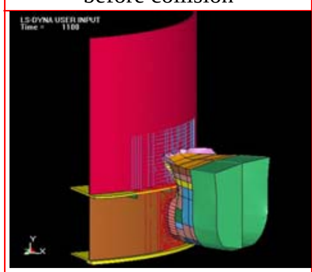

Instance C – Cellar wall initial penetration (rupture of rebar grid)

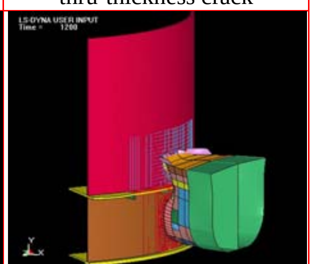

Instance D – LNG tank wall initial thru-thickness crack

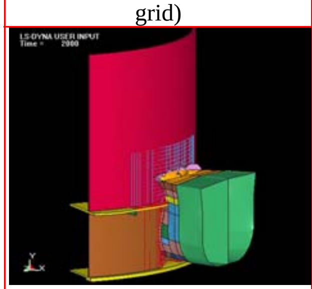

Instance E – CSC progressive damage 1

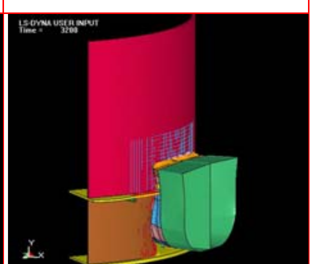

Instance F – CSC progressive damage 2

Fig. 6. CSC vs. tanker collision

The initial contact occurs at the main upper deck of the tanker, and then the bulbous section comes in contact with the cellar wall of the CSC. As the tanker is driven into the CSC structure, the CSC concrete wall at the contact areas starts to crack and spall. The tanker bulbous section is comparatively stronger than the 500 mm thick cellar wall, therefore it eventually crushes the concrete at the contact area and creates the first thru-thickness crack (Instance B of Fig. 5). After the initiation of the thru-thickness crack, the reinforcement in the concrete starts to resist most of the impact loads at the area. As the bow structure continues its path, the flare section of the bow gets in contact with the CSC cantilever walkway and is cut back locally at this interface. In the meantime, the stem of the tanker starts to buckle because of the reaction from the relatively rigid 700 mm upper tank wall. As the tanker keeps moving forward, the cellar wall reinforcement grid finally ruptures and the bulbous part of the tanker completely penetrates into the cellar compartment (Instance C). Shortly after this, the tanker stem creates cracks and crushes through the CSC tank wall and creates the first thru-thickness crack in this region (Instance D). As the tanker drives further into the CSC, the bulbous section of the tanker ruptures the reinforcement from its anchorage and creates a large opening in cellar wall (Instance E). Through the entire impact process, the CSC upper tank wall, which contains the LNG tank, behaves relatively strong and the reinforcement in this region has not ruptured at the end of simulation (Instance F).

Fig. 7 shows a snap shot of the deformed and damaged portions of the CSC and tanker bow (separated for clarity in the figure) at a late stage of the impact. Note that the stem portion of the tanker bow is completely crushed, leaving the concrete LNG tank wall with only minor damage compared to the cellar wall. Interestingly, the strong bulbous bow portion has only incurred minor damage.

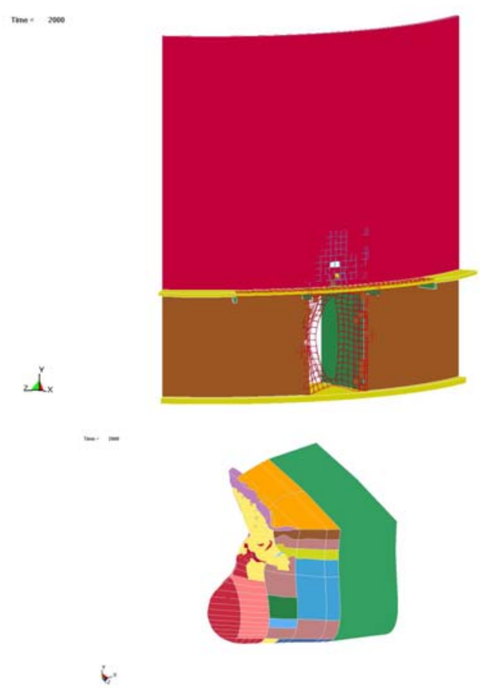

Fig. 7. Separated view of deformed and damaged tanker bow and CSC

The above internal mechanics simulation provided both the critical damage stages and the associated energy absorption. External mechanics calculations were then performed and combined with the internal mechanics simulation results to determine a relationship between the total energy dissipation and the corresponding striking tanker approaching speed. One example curve is shown in Fig. 8. In the figure, both energy and speed are normalized to those causing the worst damage to the structure (tank wall cracking for this example).

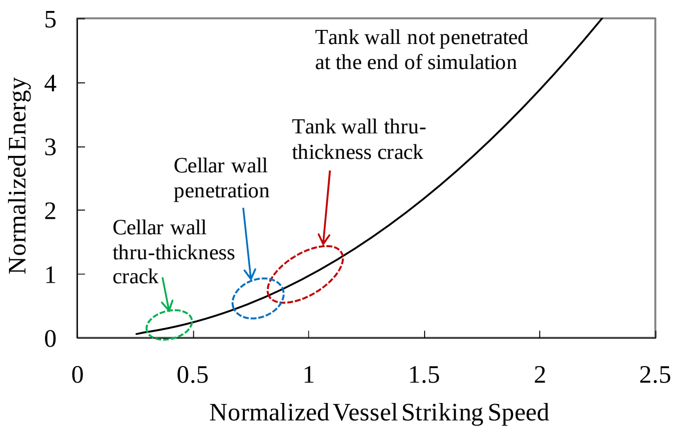

Fig. 8. Estimation of tanker striking speed and CSC damage

Fig. 8 shows that, the tanker bulbous bow may create a thru-thickness crack in the cellar wall at an approaching speed of about 0.4 normalized speed and possibly penetrate the cellar wall at about 0.8 normalized speed. The stem potion of the tanker bow may create a thru-thickness crack in the tank wall at 1.0 normalized speed. For this example case, no further damage occurs at the end of the simulated collision as all of the collision energy has been dissipated. The tank wall damage observed is insufficient to cause any LNG leak for this example. In order to perform a complete study of collisions for a facility such as this, a full suite of collision scenarios needs to be evaluated that accounts for vessel size, vessel draft, striking angle, initial vessel speed and the other specific conditions that define the CSC-vessel interface geometry and collision conditions. Fig. 8 shows results for one example case only.

CONCLUSIONS

This study takes an efficient, two-step approach to simulate the ship collision problem. The collision FEA model considers the elasto-plastic behaviors of both steel and concrete materials. Simulation results provide a reasonable evaluation of the CSC structural response to a 90^o "T-bone" impact from a representative oil trade tanker.

The simulation shows that certain collision scenarios can cause damage to both tanker bow and LNG GBS concrete structure. The damage level to the LNG GBS structure largely depends on the specific design features and arrangement of the structures involved in the collision. The ship collisions do not necessarily result in a breach of the LNG containment.

This collision simulation practice provides a practical approach to investigate the consequence of ship collision with concrete LNG GBS structures. Only one example of the many possible impact scenarios is discussed here. Other impact scenarios, such as a range of possible striking ships, different incident striking angles, drafts, impact locations etc., may produce other distinct damage conditions to the CSC. These types of cases should be investigated in order to provide a comprehensive collision study of an LNG GBS structure.

REFERENCES

Brown, A. and Chen, D., 2001. "Probabilistic method for predicting ship collision damage." Oceanic Engineering International.

El-Tawil, S., Severino, E., and Fonseca, P., 2005. "Vehicle collision with bridge piers." Journal of Bridge Engineering, Vol. 10, Issue 3, pp. 345-353.

Endo, H. and Yamada, Y., 2001. "The performance of buffer bow structures against collision (1st report: collapse strength of the simplified structure models)." Journal of the Society of Naval Architects of Japan, Vol. 189, pp. 209-217.

Jiang, D.J., Wang, G., Montaruli, B.C., and Richardson, K.L., 2004. "Concrete offshore LNG terminals, a viable solution and technical challenges." Offshore Technology Conference, OTC-16124, May 2004, Houston, Texas.

Kitamura O., 2001. "FEM approach to the simulation of collision and grounding damage." The 2nd International Conference on Collision and Grounding of Ships, Copenhagen, Denmark, July 1-3.

Kitamura, O., Kuroiwa, T., Kawamoto, Y., and Kaneko, E., 1998. "A study on the improved tanker structure against collision and grounding damage." Proceedings of the 7th PRADS, pp. 173-179.

Kuroiwa, T., 1996. "Numerical simulation of actual collision and grounding experiments." International Conference on Design and Methodologies for Collision and Grounding Protection of Ships, San Francisco.

Livermore Software Technology Corporation (LSTC), 1998. "LS-DYNA theorectical manual."

Paik J.K., Chung, J.Y., Choe, I.H., Thayamballi, A.K., Pedersen, P.T., and Wang, G., 1999. "On rational design of double hull tanker structures against collision." SNAME annual meeting, Baltimore MD, pp. 1-35.

Peterson, M.J., 1982. "Dynamics of ship collisions." Ocean Engineering, Vol. 9, No. 4, pp. 296-329.

Pedersen, P.T. and Zhang, S., 1998. "On impact mechanics in ship collisions." Marine Structures, Vol. II, pp. 429-449.

Puskar, F.J. and Litton, R.W., 1993. "Ship collision analysis for the Kawasaki island steel platforms." Offshore Technology Conference, OTC-7141, May 1993, Houston, Texas.

Simonsen, BC., 1997. "Ship grounding on rock: I & II." Marine Structures. 10:519–84.

Suzuki, K., Ohtsubo, H., and Sajit, C., 2000. "Evaluation method of absorbed energy in collision of ships with anti-collision structure." Ship Structure Symposium on Ship Structures for the New Millennium: Supporting Quality in Shipbuilding, Arlington, VA, 13-14 June.

Tornqvist, R., 2003. "Design of crashworthiness ship structures." Technical University of Denmark, Ph.D. thesis.

Wang, G., Atita, K., and Liu, D., 2000. "Behavior of a double hull in a variety of stranding or collision scenarios." Marine Structures, Vol. 13 (2000), pp.147-187.

Wang G., Jiang D.J., and Shin Y., 2003. "Consideration of collision and contact damage risks in FPSO structural designs." Offshore Technology Conference, OTC-15316. May 2003, Houston, TX.

Wierzbicki, T., 1992-1999. "Reports, joint MIT-industry program on tanker safety."

Wu, F., Spong, R., and Wang, G., 2004. "Using numerical simulation to analyze ship collision." 3rd International Conference on Collision Grounding of Ships, Izu, Japan, October 25-27.